# Comparing Spectra of Graph Shift Operator Matrices

Johannes Lutzeyer, Andrew Walden

# Comparing Spectra of Graph Shift Operator Matrices

Johannes F. Lutzeyer and Andrew T. Walden

Imperial College London, London SW7 2AZ, UK,
jl7511@ic.ac.uk, a.walden@imperial.ac.uk

**Abstract.** Typically network structures are represented by one of three different graph shift operator matrices: the adjacency matrix and unnormalised and normalised Laplacian matrices. To enable a sensible comparison of their spectral (eigenvalue) properties, an affine transform is first applied to one of them, which preserves eigengaps. Bounds, which depend on the minimum and maximum degree of the network, are given on the resulting eigenvalue differences. The monotonicity of the bounds and the structure of networks are related. Bounds, which again depend on the minimum and maximum degree of the network, are also given for normalised eigengap differences, used in spectral clustering. Results are illustrated on the karate dataset and a stochastic block model. If the degree extreme difference is large, different choices of graph shift operator matrix may give rise to disparate inference drawn from network analysis; contrariwise, smaller degree extreme difference results in consistent inference.

**Keywords:** graph shift operator matrix, spectrum, clustering

## 1 Introduction

Networks can be represented in multiple ways via different graph shift operator matrices (GSOMs), typically by the adjacency matrix or normalised or unnormalised Laplacians. The degree $d_i$ of the $i^{\text{th}}$ vertex is defined to be the sum of the weights of all edges connecting this vertex with others and the degree matrix $D$ is defined to be the diagonal matrix $D = \text{diag}(d_1, \ldots, d_n)$. With the adjacency matrix denoted by $A$, the unnormalised graph Laplacian, $L$, is defined as $L = D - A$, and there are two commonly used normalised Laplacians defined as $L_{rw} = D^{-1}L$ and $L_{sym} = D^{-1/2}LD^{-1/2}$. The aim of this work is to compare the spectra (eigenvalues) of the GSOMs, $A$ and $L$, and since the two normalised Laplacians are related by a similarity transform, so have identical eigenvalues, we choose to work with just one of these, namely $L_{rw}$.

The spectral properties of the GSOMs are utilised in many disciplines [4] for a broad range of different analysis methods, such as, the spectral clustering algorithm [17], graph wavelets [15], change point detection in dynamic networks [1] and the quantification of network similarity [7]. In particular, spectral clustering has had a big impact in the recent analysis of networks, with active research on

the theoretical guarantees which can be given for a clustering determined in this way ([11],[14]). The spectral properties of the different GSOMs are also starting to be leveraged in graph learning, as for example in [10]. It is the recommendation to use whichever GSOM works best in a particular analysis or learning task [13]. A framework under which the GSOM spectra can be compared and an improved understanding of the magnitude of the spectral differences of the GSOMs is of real use in informing such a decision.

In the remainder of the introduction we motivate the main ideas of the paper, which are the use of affine transformation to enable the comparison of the GSOM spectra, the affine transformation parameter choice and the bounds on the individual eigenvalue difference of the GSOMs. In Section 2 we provide bounds on the eigenvalue differences of the GSOMs for general graphs and visualise the effects of the affine transformation on the GSOM spectra corresponding to Zachary's karate social network. Then, in Section 3 we observe and explain the monotonicity of the eigenvalue bounds. In Section 4 we provide bounds on the difference of the normalised eigengaps (differences of successive eigenvalues) of the GSOMs and visualise them using a sample from a stochastic blockmodel. Section 5 highlights the impact of the GSOM choice on the inference drawn in graphical analysis by applying the spectral clustering algorithm using all three GSOMs to the karate network. In Section 6 we provide a summary and conclusions.

### 1.1 Motivation of the affine transformations

A direct comparison of the observed spectra is difficult. Primarily this is because for two of three comparisons to be made, the ordering of the eigenvalues is reversed; there is a rough correspondence of the *larger* end of the adjacency matrix spectrum to the the *smaller* end of the Laplacian spectra and vice versa for the other ends. Also, the supports of the three GSOM spectra are different [16, p. 29, 64, 68]. (The upcoming Figure 1 illustrates this.) For an insightful comparison it makes sense to relocate and scale the spectra (eigenvalues), $\mu_n \leq \cdots \leq \mu_1$, say, via an affine transformation $g(\mu) = c\mu + b$, where $c, b \in \mathbb{R}, c \neq 0$. Ordering is preserved for $c > 0$, i.e., $g(\mu_1) \geq g(\mu_2)$ and reversed for $c < 0$, i.e., $g(\mu_1) \leq g(\mu_2)$. Eigengaps, relative to the spectral support, are preserved. Assume the domain of $g$ is equal to the interval $[x_1, x_2]$, so $g$'s image is equal to $[g(x_1), g(x_2)]$. Then normalised eigengaps are preserved:

$$\frac{\mu_1 - \mu_2}{x_2 - x_1} = \frac{c\,(\mu_1 - \mu_2) + b - b}{c\,(x_2 - x_1) + b - b} = \frac{g(\mu_1) - g(\mu_2)}{g(x_2) - g(x_1)}. \tag{1}$$

In the spectral clustering algorithms, eigengaps are used to determine the number of clusters in the network, while the eigenvalue ordering is used to identify which eigenvectors to consider [17]. Therefore, when comparing the impact of the choice of GSOMs on graphical analysis, we need to preserve or reverse eigenvalue ordering and preserve relative eigengap size.

### 1.2 Motivation of the parameter choice

All three GSOMs are related through the degree matrix $D$. Denote the degree extremes by $d_{\min}$ and $d_{\max}$. For $d$-regular graphs, where $d_{\max} = d_{\min} = d$, the GSOMs are already exactly related by affine transformations and hence their eigenvalues are related by the same affine transformations. For general (non-$d$-regular graphs) we shall make parameter choices for the affine transformations such that eigenvalue differences, after affine transformation, can be bounded above in terms of the elements of $D$. These general parameter choices agree with the natural existing transformation parameters for $d$-regular graphs.

### 1.3 Motivation for calculating a bound on the eigenvalue differences

The motivation for bounding the eigenvalue difference is twofold. On the one hand, the structure of the bound and its dependency on network parameters allow us to infer for which graphs we are able to see larger differences in the GSOM spectra. On the other hand, the bounds allow us to add a sensible scale to observed eigenvalues; the bound represents the theoretically maximal distance the eigenvalues and eigengaps can differ by and therefore we are able to compare observed differences to the maximal possible differences.

## 2 GSOM eigenvalue differences

### 2.1 Transforms and bounds

**Theorem 1.** *Consider a graph $G$ with degree extremes $d_{\min}$ and $d_{\max}$. Let the eigenvalues of the corresponding adjacency matrix $A$ and unnormalised Laplacian matrix $L$ be denoted by $\mu_n \leq \cdots \leq \mu_1$ and $\lambda_1 \leq \cdots \leq \lambda_n$, respectively. Then, there exists a transformation $f_1(\mu_i) = c_1\mu_i + b_1$, where $c_1 = -1$ and $b_1 = (d_{\max} + d_{\min})/2$, such that for all $i \in \{1, \cdots, n\}$,*

$$|f_1(\mu_i) - \lambda_i| \leq \frac{d_{\max} - d_{\min}}{2} \stackrel{\text{def}}{=} e(A, L). \tag{2}$$

For $d$-regular graphs, (2) gives $e(A, L) = 0$, so that $f_1(\mu_i) = \lambda_i = c_1\mu_i + b_1 = d - \mu_i$, i.e., the eigenvalues are related by the required exact relation, as claimed in Section 1.2.

For general graphs, using (2), we can establish a rough correspondence, to within an affine transformation, between the eigenvalues of the adjacency matrix, $A$, and the unnormalised graph Laplacian, $L$, if the extremes of the degree sequence $d_{\max}$ and $d_{\min}$ are reasonably close.

**Theorem 2.** *Consider a graph $G$ with degree extremes $d_{\min} > 0$ and $d_{\max}$. Let the eigenvalues of $L$ and $L_{rw}$ be denoted by $\lambda_1 \leq \cdots \leq \lambda_n$ and $\eta_1 \leq \cdots \leq \eta_n$, respectively. Then, there exists a transformation $f_2(\lambda_i) = c_2\lambda_i + b_2$, where $c_2 = 2/(d_{\max} + d_{\min})$ and $b_2 = 0$, such that for all $i \in \{1, \cdots, n\}$,*

$$|f_2(\lambda_i) - \eta_i| \leq 2\,\frac{d_{\max} - d_{\min}}{d_{\max} + d_{\min}} \stackrel{\text{def}}{=} e\,(L, L_{rw})\,. \tag{3}$$

Asymptotically, as $d_{\max} \to \infty$ with fixed $d_{\min} > 0$, the bound $e\left(L, L_{rw}\right)$ tends to 2. The restricted range of $d_{\min}$ is due to $D^{-1}$, the normalised Laplacian and consequently the bound $e(L, L_{rw})$ not being defined for $d_{\min} = 0$. For $d$-regular graphs, where $d_{\max} = d_{\min} = d$, the bound equals zero. Hence, the spectra of $f_2(L)$ and $L_{rw}$ are equal and $\eta_i = c_2\lambda_i = \lambda_i/d$, i.e., the eigenvalues are related by the required exact relation. Overall, the behaviour of this bound is similar to $e(A, L)$. The smaller the difference of the degree sequence extremes $d_{\max}$ and $d_{\min}$, the closer the spectra of $L$ and $L_{rw}$ are related, signified by a smaller bound on the eigenvalue differences.

**Theorem 3.** *Consider a graph $G$ with degree extremes $d_{\min} > 0$ and $d_{\max}$. Let the eigenvalues of $A$ and $L_{rw}$ be denoted by $\mu_n \leq \cdots \leq \mu_1$ and $\eta_1 \leq \cdots \leq \eta_n$, respectively. Then, there exists a transformation $f_3(\mu_i) = c_3\mu_i + b_3$, where $c_3 = -2/(d_{\max} + d_{\min})$ and $b_3 = 1$, such that for all $i \in \{1, \cdots, n\}$,*

$$|f_3(\mu_i) - \eta_i| \leq \frac{d_{\max} - d_{\min}}{d_{\max} + d_{\min}} \stackrel{\text{def}}{=} e\left(A, L_{rw}\right). \tag{4}$$

For $d$-regular graphs, $e\left(A, L_{rw}\right)$ equals zero and hence the spectra of $f_3(A)$ and $L_{rw}$ are equal and $\eta_i = 1 + c_3\mu_i = 1 - (\mu_i/d)$, i.e., the spectra of $L_{rw}$ and $A$ are related by the required exact relation. For general graphs, $e(A, L_{rw})$ is small for small degree extreme differences and hence the spectra of the two GSOMs exhibit smaller maximal differences, as was the case for $e(A, L)$ and $e(L, L_{rw})$.

The proofs of Theorems 1, 2 and 3 directly follow from inequality (4.3) in [2, p. 46], choosing parameters $c_1, b_2$ and $b_3$ as given in the theorem statements to make the problem analytically solvable and by then analytically minimising the two norm. More detailed proofs of the theorems are available from the authors upon request.

### 2.2 Karate dataset example

The karate dataset [3] dates back to [19]. We work with a square matrix with 34 entries, '`ZACHE`,' which is the adjacency matrix of a social network describing presence of interaction in a university karate club. This data set is popular as it naturally lends itself to clustering [5, 8, 9].

The untransformed and transformed eigenvalues of the GSOMs $A$, $L$ and $L_{rw}$ of Zachary's karate dataset are shown in Figure 1. From Figs. 1(a), (b) and (c) not much can be said about how the spectra compare. From Figs. 1(d), (e) and (f) it can be observed that each pair of spectra of the karate dataset cover a similar range after transformation and that clearly the spectra of $A$ and $L_{rw}$ are the most similar of the three. It can also be seen that the largest eigengaps occur at opposing ends of the spectra when comparing $A$ and $L_{rw}$ with $L$. This observation is only possible from the plots including the transforms, i.e., Figs. 1(d), (e) and (f). Clearly, the eigenvalue spectra become more comparable through utilising the proposed transformations.

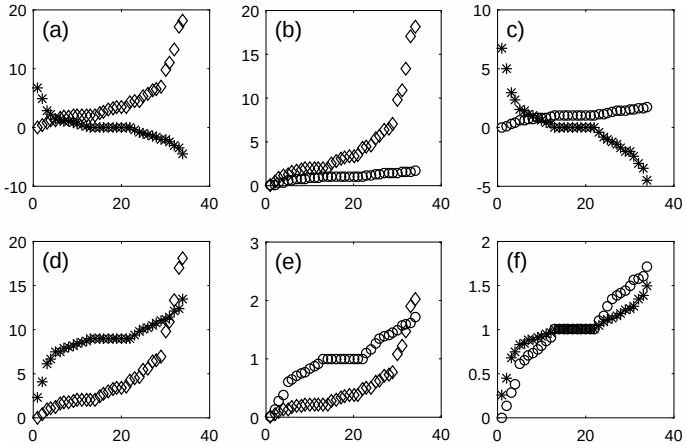


**Fig. 1.** Transformation results for Zachary's karate dataset. First row: (a) eigenvalues $\mu$ of $A$ (stars) and $\lambda$ of $L$ (diamonds); (b) eigenvalues $\lambda$ of $L$ and $\eta$ of $L_{rw}$ (circles); (c) eigenvalues $\mu$ of $A$ and $\eta$ of $L_{rw}$. Second row: the first of the two eigenvalue spectra are transformed by their respective transformations $f_1, f_2$ and $f_3$.

*Remark 1.* [20, p. 32] shows that vertices with identical neighbourhoods generate eigenvalues equal to 0 and 1 in the adjacency and normalised Laplacian spectrum, respectively. Interestingly, we spot several such vertices in the karate network, which will be shown in Fig. 4, and several corresponding eigenvalues equal to 0 and 1 in Fig. 1(c). It is very nice to see that the equivalence of these eigenvalues is highlighted by our transformation mapping them exactly onto each other in Fig. 1(f). ◁

In Fig. 2, we display a proof of concept of our bounds. The eigenvalue bounds are centred around the average value of each eigenvalue pair in order to highlight the maximal difference achievable by each individual eigenvalue pair under comparison. For the karate dataset the bound values $(e(A,L), e(L,L_{rw}), e(A,L_{rw}))$ are equal to $(8.00, 1.78, 0.89)$. The particular bounds displayed here are valid for all graphs with $d_{\min} = 1$ and $d_{\max} = 17$, i.e., all graphs in $\mathcal{C}_{1,17}$, where $\mathcal{C}_{j,k}$ is the class of graphs with $d_{\min} = j$ and $d_{\max} = k$. The bounds being almost attained in plot (a), and not attained in plots (b) and (c), is more a consequence of the structure of the graph given by the karate data set than tightness and quality of the bounds. Since the three bounds $e(A,L)$, $e(L,L_{rw})$ and $e(A,L_{rw})$ apply to entire classes $\mathcal{C}_{j,k}$ at a time, we can only achieve tightness on these classes — bounds being attained for some elements in $\mathcal{C}_{j,k}$ — and not on each individual element of them.

So for our particular social network, the karate dataset, firstly the bound being almost attained in plot (a) tells us that the spectra of $A$ and $L$ deviate almost as much as theoretically possible for a graph in $\mathcal{C}_{1,17}$. Secondly, from plot (c) we see that the spectra of $A$ and $L_{rw}$ are rather similar for the karate data

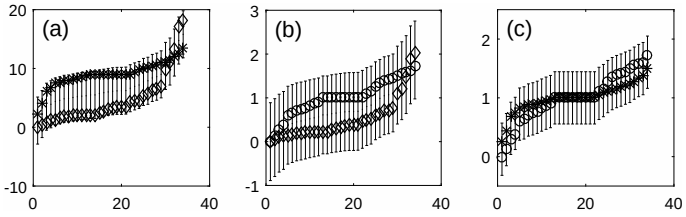


**Fig. 2.** Eigenvalue bounds on the karate eigenvalues. In plot (a) we display the bound $e(A, L)$ via the intervals together with the transformed eigenvalues of the adjacency matrix $f_1(\mu)$ (stars) and the eigenvalues of the Laplacian $\lambda$ (diamonds). (b) the bound $e(L, L_{rw})$ is displayed via the intervals, the diamonds correspond to the transformed Laplacian eigenvalues $f_2(\lambda)$ and the circles are the eigenvalues of the normalised graph Laplacian $\eta$. (c) the bound $e(A, L_{rw})$ is displayed via the intervals, the stars correspond to the transformed adjacency eigenvalues $f_3(\mu)$ and the circles are the normalised Laplacian eigenvalues $\eta$.

**Table 1.** Comparing bounds on eigenvalue differences of $A, L$ and $L_{rw}$. The bound values are displayed as $(e(A, L), e(L, L_{rw}), e(A, L_{rw}))$.

| | $d_{\min}$ | | | | |
|---|---|---|---|---|---|
| | 0 | 1 | 2 | 3 | 4 |
| 1 | ( 0.5, ·, ·) | ( 0, 0, 0) | * | * | * |
| 2 | ( 1, ·, ·) | ( 0.5, 0.67, 0.33) | ( 0, 0, 0) | * | * |
| 3 | ( 1.5, ·, ·) | (1, 1, 0.5) | ( 0.5, 0.4, 0.2) | ( 0, 0, 0) | * |
| $d_{\max}$ 4 | (2, ·, ·) | ( 1.5, 1.2, 0.6) | ( 1, 0.67, 0.33) | (0.5, 0.29, 0.14) | ( 0, 0, 0) |
| 5 | ( 2.5, ·, ·) | ( 2, 1.33, 0.67) | (1.5, 0.86, 0.43) | (1, 0.5, 0.25) | (0.5, 0.22,0.11) |
| 6 | ( 3, ·, ·) | (2.5, 1.43, 0.71) | (2, 1, 0.5) | (1.5, 0.67, 0.33) | (1, 0.4, 0.2) |

set and could theoretically deviate significantly more for a different graph in $\mathcal{C}_{1,17}$ having degree extreme difference 16. The bounds give us insight into how particular GSOM spectra behave for the karate dataset.

## 3 Relating the spectral bounds

We display some sample bound values in Table 1. The first column of Table 1 only contains values of $e(A, L)$ as for $d_{\min} = 0$ the normalised Laplacian and hence $e(L, L_{rw})$ and $e(A, L_{rw})$ are not well-defined. In practice this is of little consequence since disconnected nodes are commonly removed from the dataset as a preprocessing step. On the diagonal of Table 1, where $d_{\max} = d_{\min}$, i.e., for the $d$-regular graphs, we find $e(A, L) = e(L, L_{rw}) = e(A, L_{rw}) = 0$ due to the direct spectral relation of the GSOMs.

*Remark 2.* It is interesting to note, that since the spectral support of neither $A$, nor $L$, is bounded, the bound on their eigenvalue difference is also not bounded above. (This explains the large values in Fig. 2(a)). This does not apply to the other two bounds as we have $e\left(L, L_{rw}\right) \leq 2$ and $e\left(A, L_{rw}\right) \leq 1$. ◁

Before discussing the structure of Table 1, we define connected components in a graph.

**Definition 1.** *A path on a graph $G$ is an ordered list of unique vertices such that consecutive vertices are connected by an edge. A vertex set $S_k$ is called a connected component if there exists a path between any two vertices $v_i, v_j \in S_k$ and there exists no path from any $v_i \in S_k$ to any $v_j \notin S_k$.* ◁

Since all graphs in $\mathcal{C}_{j+1,k}$ can be extended to lie in $\mathcal{C}_{j,k}$ by adding one or more connected components, all spectra of graphs in $\mathcal{C}_{j+1,k}$ are subsets of spectra of graphs in $\mathcal{C}_{j,k}$ (the GSOM spectrum of a graph is the union of the spectra of its connected components [6, p. 7]). Therefore, the support of the spectra of graphs in $\mathcal{C}_{j,k}$ must be larger or equal to the support of spectra of graphs in $\mathcal{C}_{j+1,k}$. Hence, we expect the spectral bounds, $e(\cdot,\cdot)$, we derived to be decreasing or constant with increasing $d_{\min}$ and constant $d_{\max}$. This phenomenon can be observed in Table 1 when traversing each *row*.

In similar fashion, any graph in $\mathcal{C}_{j,k}$, can be extended to be a graph in $\mathcal{C}_{j,k+1}$, by adding a connected component with all vertex degrees greater or equal to $j$ and smaller or equal than $k{+}1$ with at least one node attaining degree $k{+}1$. Then spectra of graphs in $\mathcal{C}_{j,k}$ are subsets of spectra of graphs $\mathcal{C}_{j,k+1}$ and therefore the spectral support and hence the spectral bounds on $\mathcal{C}_{j,k+1}$ have to be greater or equal than the respective quantities for $\mathcal{C}_{j,k}$. So, any of the spectral bounds, $e(\cdot,\cdot)$, will be increasing or constant with increasing $d_{\max}$ and constant $d_{\min}$, as seen in the *columns* of Table 1.

## 4 GSOM normalised eigengap differences

Here we derive bounds on the normalised eigengap differences, where each eigengap is normalised by the spectral support of its corresponding GSOM.

### 4.1 Normalised eigengap difference of $A$ and $L$

Let $\mathcal{M}_i$ denote the $i^{\text{th}}$ eigengap of $A$, $\mathcal{M}_i = \mu_i - \mu_{i+1}$, $\mathcal{L}_i$ denote the $i^{\text{th}}$ eigengap of $L$, $\mathcal{L}_i = \lambda_{i+1} - \lambda_i$ and $\mathcal{N}_i$ denote the $i^{\text{th}}$ eigengap of $L_{rw}$, $\mathcal{N}_i = \eta_{i+1} - \eta_i$, for $i \in \{1, 2, \ldots, n-1\}$. The spectral supports of $A$, $L$ and $L_{rw}$ are equal to $[-d_{\max}, d_{\max}]$, $[0, 2d_{\max}]$ and $[0, 2]$, respectively [16, p. 29,64,68], so the lengths of the supports are $\ell(\mu) = \ell(\lambda) = 2d_{\max}$ and $\ell(\eta) = 2$.

From (1) we see that the normalisation of transformed eigengaps by the transformed spectral support is equal to the normalisation of the untransformed eigengaps by the untransformed spectral support. We will therefore start our analysis by considering the untransformed normalised eigengaps. Eigengap normalisation by the spectral support of the corresponding GSOM is crucial to be able to make a meaningful comparison of eigengap magnitudes.

**Theorem 4.** *Bounds on the normalised eigengap difference of the GSOMs are given by*

$$\left|\frac{\mathcal{M}_i}{2d_{\max}} - \frac{\mathcal{L}_i}{2d_{\max}}\right| \leq \frac{d_{\max} - d_{\min}}{2d_{\max}} \stackrel{\text{def}}{=} g(A, L);$$
$$\left|\frac{\mathcal{L}_i}{2d_{\max}} - \frac{\mathcal{N}_i}{2}\right| \leq 2\frac{d_{\max} - d_{\min}}{d_{\max}} \stackrel{\text{def}}{=} g(L, L_{rw});$$
$$\left|\frac{\mathcal{M}_i}{2d_{\max}} - \frac{\mathcal{N}_i}{2}\right| \leq \frac{d_{\max} - d_{\min}}{d_{\max}} \stackrel{\text{def}}{=} g(A, L_{rw}).$$

The proofs of the three inequalities in Theorem 4 directly follow by applying the triangle inequality and then varying the proofs of Theorems 1, 2 and 3 slightly to accommodate the normalisation of the spectra as transformation parameters. More detailed proofs of the theorems are available from the authors upon request.

### 4.2 Stochastic blockmodel example

Throughout this section we interpret large eigengaps in the context of spectral clustering. Firstly, large eigengaps are understood to indicate the number of clusters discovered by the different GSOMs, i.e., a large $K^{\text{th}}$ eigengap is understood to indicate a clustering into $K$ communities [17, p. 410]. Secondly, the size of the eigengap is understood to represent relative strength of evidence for a certain clustering [17, p. 407].

We see that the eigengaps of the GSOMs are different, giving further evidence that the graphical structure captured in the different spectra differs significantly and possibly in a structured manner. Furthermore, we have been able to use our bounds to put the magnitude of the observed eigengaps into the broader perspective of all graphs with corresponding degree extremes.

The stochastic blockmodel, which is widely used in the networks literature [9, 11], allows us to encode a block structure in a random graph via different probabilities of edges within and between node-blocks. Our definition and parametrisation is adapted from [11].

**Definition 2.** *Consider a graph with node set $\{v_1, \ldots, v_n\}$. Split this node set into $K$ disjoint blocks denoted $\mathcal{B}_1, \ldots, \mathcal{B}_K$. We encode block membership of the nodes via a membership matrix $M \in \{0,1\}^{n\times K}$, where $M_{i,j} = 1$ if $v_i \in \mathcal{B}_j$ and $M_{ij} = 0$ otherwise. Finally, we fix the probability of edges between blocks to be constant and collect these probabilities in a probability matrix $P \in [0,1]^{K\times K}$, i.e., for nodes $v_i \in \mathcal{B}_l$ and $v_j \in \mathcal{B}_m$ the probability of an edge between $v_i$ and $v_j$ is equal to $P_{l,m}$.* ◁

Hence, the parameters of the stochastic blockmodel are $M \in \{0,1\}^{n\times K}$ and $P \in [0,1]^{K\times K}$, where the number of nodes $n \in \mathbb{N}$ and the number of clusters $K \in \mathbb{N}$ are implicitly defined via the dimensions of $M$. We simulate graphs from this model by fixing these parameters and then sampling edges from Bernoulli trials. The Bernoulli parameter of the trial corresponding to the edge connecting $v_i$ to $v_j$ is given by the $(i,j)^{\text{th}}$-entry of the matrix $MPM^T$.

Figure 3 contains eigengaps corresponding to the three GSOMs of a graph arising as a realisation of a stochastic blockmodel with parameters $n = 600$; $K = 6$; $M_{1,1} = \ldots = M_{100,1} = M_{101,2} = \ldots = M_{200,2} = M_{201,3} = \ldots = M_{300,3} = M_{301,4} = \ldots = M_{400,4} = M_{501,6} = \ldots = M_{600,6} = 1$ and all other entries of $M$ equal 0;

$$P = \begin{pmatrix} 0.9 & 0.1 & 0.1 & 0 & 0 & 0 \\ 0.1 & 0.9 & 0.1 & 0 & 0 & 0 \\ 0.1 & 0.1 & 0.9 & 0 & 0 & 0 \\ 0 & 0 & 0 & 0.1 & 0.9 & 0.9 \\ 0 & 0 & 0 & 0.9 & 0.1 & 0.9 \\ 0 & 0 & 0 & 0.9 & 0.9 & 0.1 \end{pmatrix}.$$

Hence, we have a network of 6 blocks with 100 nodes per block. From observation of $P$, we recognise that all realisations from this model consist of at least *two connected components* since the probability of an edge between blocks $\{\mathcal{B}_1, \mathcal{B}_2, \mathcal{B}_3\}$ and $\{\mathcal{B}_4, \mathcal{B}_5, \mathcal{B}_6\}$ is equal to 0.

In order to gain more insight into the block structure of this stochastic blockmodel we consider different definitions of clusters or blocks. [14] describe so called '*heterophilic*' clusters, which they recover from the eigenvectors corresponding to the extreme negative eigenvalues of the normalised Laplacian. These heterophilic clusters have fewer connections within than between clusters and are exemplified by romantic relationship graphs where the genders are the two biggest clusters identifiable. Our blockmodel includes such heterophilic blocks in $\{\mathcal{B}_4, \mathcal{B}_5, \mathcal{B}_6\}$. While blocks $\{\mathcal{B}_1, \mathcal{B}_2, \mathcal{B}_3\}$ form clusters in the more traditional sense with more edges within rather than between blocks, which will be referred to as '*homophilic*' cluster structure for the remainder of this analysis.

In Figure 3 we find that all three spectra have a non-zero normalised eigengap with indices 2, 4 and 598. In addition, $A$ has a large first normalised eigengap and $L$ a large $301^{\text{st}}$ normalised eigengap; with the exception of these two large eigengaps, in the context of the spectral clustering algorithms the eigengaps suggest searching for similar numbers of clusters.

From [17, p. 397,398] we know that the nonzero second eigengap of the Laplacians in Figure 3 encodes the separation of the network into two connected components. It is interesting to see that all GSOMs put higher weight on the block structure encoded in the stochastic blockmodel which corresponds to the large $4^{\text{th}}$ and $598^{\text{th}}$ normalised eigengaps each suggesting the search for the block structure encoded mainly in one of the two connected components of our stochastic blockmodel. It is especially interesting that for $A$ and $L$ the $4^{\text{th}}$ and $598^{\text{th}}$ normalised eigengaps are approximately equal, while for $L_{rw}$ the $4^{\text{th}}$ normalised eigengap is almost twice as large as the $598^{\text{th}}$ normalised eigengap. Both components have symmetric parameters and therefore it is very interesting that the eigengaps in $L_{rw}$ suggest stronger evidence for the homophilic cluster structure encoded by the $4^{\text{th}}$ eigengap rather than the heterophilic cluster structure encoded by the $598^{\text{th}}$ eigengap. A much larger simulation of stochastic blockmodels with varying parameters, which is beyond the scope of this work, could establish whether $L_{rw}$ does indeed have a structured preference for homophilic over heterophilic blocks.

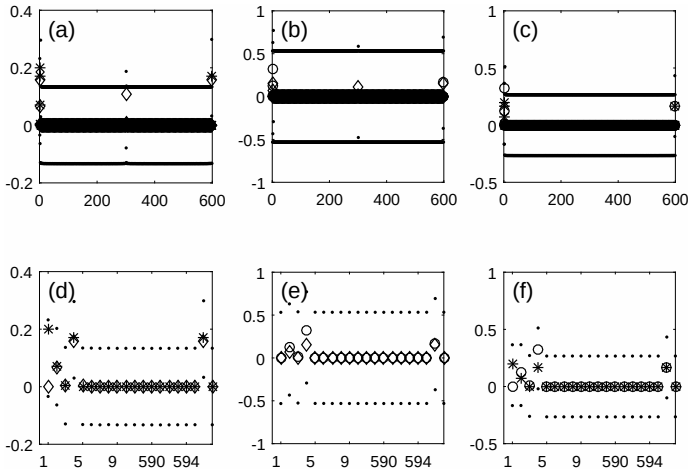


**Fig. 3.** Plots (a), (b) and (c) display all normalised eigengaps and plots (d), (e) and (f) display the first and last 10 normalised eigengaps of a graph sampled from a stochastic blockmodel. The stars correspond to eigengaps of $A$ normalised by the spectral support of $A$, the diamonds display the corresponding quantity for $L$ and the circles represent the corresponding quantity for $L_{rw}$. The solid black dots correspond to the three bounds, where $g(A, L)$ is displayed in plots (a) and (d), $g(L, L_{rw})$ is shown in plots (b) and (e) and $g(A, L_{rw})$ is displayed in plots (c) and (f).

## 5 Application to spectral clustering

To illustrate the impact of the GSOM choice, we display the spectral clustering according to the first two eigenvectors of each of the three GSOMs corresponding to the karate data set. The choice of GSOM has a significant impact on the clustering outcome. We use the simplest form of spectral clustering by running the $k$-means algorithm on the rows of the first $k$ eigenvectors of the different GSOMs [17, p. 399].

Since for the karate dataset, we have a reasonably large degree extreme difference, $d_{\max} - d_{\min} = 16$, we expect to see deviating results in the spectral clustering according to the different GSOMs.

At first sight, all clusterings displayed in Figure 4 seem sensible. The clustering according to the adjacency matrix extends the cluster marked with the unfilled, square nodes by one node, karate club member 3, in comparison to the clustering according to the normalised Laplacian. In contrast, the unnormalised Laplacian detects 5 nodes less (karate club members 2, 4, 8, 14 and 20) in the cluster marked by the unfilled square nodes, than does the normalised Laplacian.

We find the clustering according to the adjacency matrix $A$ to agree with the true clustering suggested by the eventual split of the karate club as recorded by [19]. The normalised Laplacians misplace one out of 34 nodes, which is known to be difficult to cluster correctly in the literature [8]. The unnormalised Laplacian

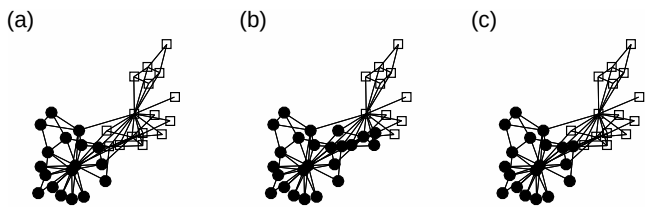


**Fig. 4.** Spectral clustering of the karate network according to the first two eigenvectors of the adjacency matrix $A$ in (a), the unnormalised Laplacian $L$ in (b) and the normalised Laplacian $L_{rw}$ in (c).

however, misplaces 6 nodes, only one of which is known to us to be commonly misclustered. Hence, the unnormalised Laplacian clustering is clearly outperformed by the other two GSOMs when using the first two eigenvectors to find two communities in the karate data set. In [18] the conditions under which spectral clustering using the unnormalised Laplacian converges are shown to be more restrictive than the conditions under which spectral clustering according to the normalised Laplacian converges. [18] hence advocate using the normalised Laplacian for spectral clustering over the unnormalised Laplacian. Our clustering results agree with this recommendation.

*Remark 3.* The choice of GSOM can clearly impact the results of cluster inference via spectral clustering. We suggest considering the degree extreme difference as a parameter in graphical signal processing to infer the potential impact of the choice of GSOM. ◁

## 6 Summary and Conclusions

We have compared the spectra of the GSOMs: the adjacency matrix $A$, the unnormalised graph Laplacian $L$ and the normalised graph Laplacian $L_{rw}$ and found differences in the spectra corresponding to general graphs. For all three pairs of GSOMs the degree extreme difference, $d_{\max} - d_{\min}$, was found to linearly upper bound both the spectral differences, when transforming one of the two spectra by an affine transformation, and the normalised eigengap differences. We explained the monotonicity found in the eigenvalue bounds by partitioning the class of graphs according to their degree extremes and considering the addition/deletion of connected components to/from the graph. Our bounds were illustrated on Zachary's karate network and on a network sampled from a stochastic blockmodel with homophilic and heterophilic cluster structures. *We find that if the degree extreme difference is large, different choices of GSOMs may give rise to disparate inference drawn from network analysis; smaller degree extreme differences will result in consistent inference, whatever the choice of GSOM.* The significant differences in inference drawn from graphical analysis using the different GSOMs were illustrated via the spectral clustering algorithm applied to Zachary's karate network.

## References


1. Aleardi, L.C., Salihoglu, S., Singh, G., Ovsjanikov, M.: Spectral Measures of Distortion for Change Detection in Dynamic Graphs In: Aiello, L.M., Cherifi, C., Cherifi, H., Lambiotte, R., Lió, P., Rocha, L.M. (eds) Complex Networks and Their Applications VII, pp. 54–66, Springer (2019). doi:10.1007/978-3-030-05414-4_5
2. Bai, Z., Demmel, J., Dongarra, J., Ruhe, A., van der Vorst, H.: Templates for the solution of algebraic eigenvalue problems: a practical guide. SIAM (2000).
3. Batagelj, V., Mrvar, A.: Pajek datasets, http://vlado.fmf.uni-lj.si/pub/networks/data/ (2006). Accessed: 2016-11-23
4. Cvetkovic, D., Gutman, I.: Applications of graph spectra: An introduction to the literature. Zbornik radova, vol. 14, pp. 9–34 (2011).
5. Chen, P.Y., Hero,A.O.: Deep community detection. IEEE Trans. Signal Process. vol. 63, pp. 5706–5719 (2015). doi:10.1109/TSP.2015.2458782
6. Chung, F.R.K.: Spectral graph theory. American Mathematical Soc. (1997).
7. Crawford, B., Gera, R., House, J.,Knuth, T., Miller, R.: Graph Structure Similarity using Spectral Graph Theory In: Cherifi, H., Gaito, S., Quattrociocchi, W.,Sala, A. (eds) Complex Networks & Their Applications V, pp. 209–221, Springer (2017). doi:10.1007/978-3-319-50901-3_17
8. Fortunato, S.: Community detection in graphs. Phys. Rep., vol. 486, pp. 75–174 (2010). doi:10.1016/j.physrep.2009.11.002
9. Karrer, B., Newman, M.E.J.: Stochastic blockmodels and community structure in networks. Phys. Rev. E, vol. 83, pp. 016107 (2011). doi:10.1103/PhysRevE.83.016107
10. Kumar, S., Ying, J., Cardoso, J.V. de M., Palomar, D.P.: A Unified Framework for Structured Graph Learning via Spectral Constraints. arXiv:1904.09792 [stat.ML] (2019).
11. Lei, J., Rinaldo, A.: Consistency of spectral clustering in stochastic block models. Ann. Stat., vol. 43, pp. 215–237 (2015). doi:10.1214/14-AOS1274
12. Lutzeyer, J.F., Walden, A.T.: Comparing Spectra of Graph Shift Operator Matrices. In: Cherifi, H., Gaito, S., Mendes, J.F., Moro, E., Rocha, L.M. (eds.) Complex Networks and Their Applications VIII, pp. 191–202. Springer, Cham (2020). https://doi.org/10.1007/978-3-030-36683-4_16
13. Ortega, A., Frossard, P., Kovacevic, J., Moura, J.M.F., Vandergheynst, P.: Graph Signal Processing: Overview, Challenges, and Applications. Proc. IEEE, vol. 106, pp. 808–828 (2018). doi:10.1109/JPROC.2018.2820126
14. Rohe, K., Chatterjee, S., Yu, B.: Spectral clustering and the high-dimensional stochastic blockmodel. Ann. Stat., vol. 39, pp. 1878–1915 (2011). doi:10.1214/11-AOS887
15. Tremblay, N., Borgnat, P.: Graph wavelets for multiscale community mining. IEEE Signal Process. Mag., vol. 62, pp. 5227–5239 (2014). doi:10.1109/TSP.2014.2345355
16. van Mieghem, P.: Graph Spectra for Complex Networks. Cambridge University Press, Cambridge U.K. (2011).
17. von Luxburg, U.: A tutorial on spectral clustering. Stat. Comput., vol. 17, pp. 395–416 (2007). doi:10.1109/TSP.2015.2458782
18. von Luxburg, U., Belkin, M., Bousquet, O.: Consistency of spectral clustering. Ann. Stat., vol. 36, pp. 555–586 (2008). doi:10.1214/009053607000000640
19. Zachary, W.W.: An information flow model for conflict and fission in small groups. J. Anthropol. Res., vol. 33, pp. 452–473 (1977). doi:10.1086/jar.33.4.3629752
20. Zumstein, P., Comparison of Spectral Methods Through the Adjacency Matrix and the Laplacian of a Graph. PhD thesis, ETH Zürich (2005).

# Proofs of the Theorems in "Comparing Spectra of Graph Shift Operator Matrices"

Johannes F. Lutzeyer and Andrew T. Walden

Imperial College London, London SW7 2AZ, UK,
jl7511@ic.ac.uk, a.walden@imperial.ac.uk

In this document we present detailed proofs of all theorems contained in [3].

## 1 Notation

We follow the notation in [3], which will be recalled in this section. We work with undirected, simple graphs with $n$ nodes, in which the number of edges connected to the $i^{\text{th}}$ vertex is denoted by $d_i$. Then, we are able to define the diagonal degree matrix $D = \text{diag}(d_1, \dots, d_n)$. We denote the maximal and minimal degree in a graph by $d_{\max}$ and $d_{\min}$, respectively. From the degree matrix follow the definitions of the three graph shift operator matrices (GSOMs) considered in this document, namely, the adjacency matrix $A$, the unnormalised Laplacian $L = D - A$ and the normalised Laplacian $L_{rw} = D^{-1}L$. We denote the spectra (eigenvalues) of $A$, $L$ and $L_{rw}$ by $\mu_n \leq \dots \leq \mu_1$, $\lambda_1 \leq \dots \leq \lambda_n$ and $\eta_1 \leq \dots \leq \eta_n$, respectively. From the GSOM spectra we are able to define the eigengaps of $A$, $L$ and $L_{rw}$ as $\mathcal{M}_i = \mu_i - \mu_{i+1}$, $\mathcal{L}_i = \lambda_{i+1} - \lambda_i$, $\mathcal{N}_i = \eta_{i+1} - \eta_i$, respectively, for $i \in \{1, 2, \dots, n-1\}$.

## 2 Proof of Theorem 1

*Proof.* From [2, p. 385] it follows that $f_1(A) = c_1 A + b_1 I$ has eigenvalues of the form,

$$f_1(\mu_i) = c_1 \mu_i + b_1. \tag{1}$$

Now, we proceed to analyse the error made by approximating $\lambda_i$ by $f_1(\mu_i)$. Here we view the affine transform $f_1(A)$ as a perturbation of $L$. Firstly, using inequality (4.3) in [1, p. 46],

$$\|f_1(A) - L\|_2 \geq |f_1(\mu_i) - \lambda_i| = |c_1\mu_i + b_1 - \lambda_i|, \tag{2}$$

for $i \in \{1, 2, \dots, n\}$ and $c_1 \leq 0$ (to ensure equal ordering in magnitude of the two compared spectra). In other words, the difference of corresponding eigenvalues of a symmetric matrix $L$ and its 'perturbed' version $f_1(A)$ is bounded by the two norm of the perturbation $f_1(A) - L$. Now,

$$\|f_1(A) - L\|_2 = \|b_1 I - D + (1 + c_1)A\|_2 . \tag{3}$$

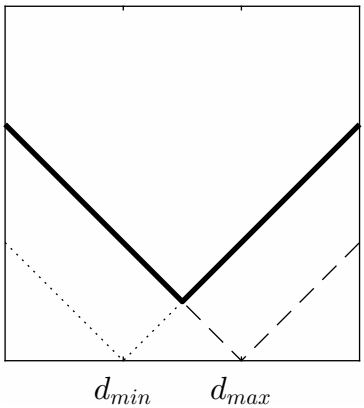


**Fig. 1.** This plot displays values of $b_1$ on the x-axis. The dotted line corresponds to the function $|d_{\min} - b_1|$, the dashed line plots the function $|d_{\max} - b_1|$ and the solid line depicts the bound which is to be minimised in (4), i.e., $\max(|d_{\max} - b_1|, |d_{\min} - b_1|)$.

We are able to reexpress this norm in a simple form in terms of $D$ by the choice $c_1 \stackrel{\text{def}}{=} -1$, i.e.,

$$\begin{aligned} \|f_1(A) - L\|_2 &= \|b_1 I - D\|_2 \\ &= \max\left(|b_1 - d_{\max}|, |b_1 - d_{\min}|\right). \end{aligned} \tag{4}$$

Equation (4) uses the fact that the eigenvalues of diagonal matrices are equal to their diagonal elements. From Fig. 1 it is obvious that (4) is analytically minimised at the intersection of the increasing part of the dotted line, $|d_{\min} - b_1|$, and the decreasing part of the dashed line, $|d_{\max} - b_1|$, which is calculated now.

$$\begin{aligned} b_1 - d_{\min} &= d_{\max} - b_1 \\ \Leftrightarrow b_1 &= \frac{d_{\max} + d_{\min}}{2}. \end{aligned}$$

Evaluating (4) at $b_1 \stackrel{\text{def}}{=} (d_{\max} + d_{\min})/2$ gives,

$$\|f_1(A) - L\|_2 = \frac{d_{\max} - d_{\min}}{2}.$$

Putting (2) and (4) together, we obtain

$$|f_1(\mu_i) - \lambda_i| \leq \frac{d_{\max} - d_{\min}}{2} \stackrel{\text{def}}{=} e(A, L).$$

## 3 Proof of Theorem 2

*Proof.* As in the proof of Theorem 1, $f_2(L) = c_2 L + b_2 I$ has eigenvalues of the form,

$$f_2(\lambda_i) = c_2 \lambda_i + b_2. \tag{5}$$

The following result is the equivalent of (2):

$$\|f_2(L) - L_{rw}\|_2 \geq |f_2(\lambda_i) - \eta_i\ | = |c_2\lambda_i + b_2 - \eta_i|\,, \tag{6}$$

for $i \in \{1, 2, \ldots, n\}$ and $c_2 \geq 0$ (to ensure equal ordering in magnitude of the two compared spectra). In the steps that follow we use firstly that the eigenvalues of $L_{rw}$ are all positive, and secondly that $\|L_{rw}\|_2 \leq 2$; as established in [4, p. 64]. Now,

$$\|f_2(L) - L_{rw}\|_2 = \|(c_2 D - I)\, L_{rw} + b_2 I\|_2\,.$$

The norm can be simplified by the choice $b_2 = 0$, i.e.,

$$\begin{aligned} \|f_2(L) - L_{rw}\|_2 &= \|(c_2 D - I)\, L_{rw}\|_2 &(7)\\ &\leq \|L_{rw}\|_2\, \|c_2 D - I\|_2 \\ &\leq 2 \max\left(|d_{\max} c_2 - 1|\,, |d_{\min} c_2 - 1|\right). &(8)\end{aligned}$$

From Fig. 2 it is obvious that (8) is analytically minimised at the intersection of the increasing part of the dashed line, $|d_{\max} c_2 - 1|$, and decreasing part of the dotted line, $|d_{\min} c_2 - 1|$, which is calculated now.

$$\begin{aligned} & d_{\max} c_2 - 1 = -\left(d_{\min} c_2 - 1\right) \\ \Leftrightarrow\ & \left(d_{\max} + d_{\min}\right) c_2 = 2 \\ \Leftrightarrow\ & c_2 = \frac{2}{d_{\max} + d_{\min}}. \end{aligned}$$

Evaluating (8) at $c_2 \stackrel{\text{def}}{=} 2/(d_{\max} + d_{\min}) = 1/b_1$ gives,

$$\|f_2(L) - L_{rw}\|_2 \leq 2\, \frac{d_{\max} - d_{\min}}{d_{\max} + d_{\min}}.$$

We thus obtain

$$|f_2(\lambda_i) - \eta_i| \leq 2\, \frac{d_{\max} - d_{\min}}{d_{\max} + d_{\min}} \stackrel{\text{def}}{=} e\left(L, L_{rw}\right).$$

## 4 Proof of Theorem 3

*Proof.* As in the proof of Theorems 1 and 2, $f_3(A) = c_3 A + b_3 I$ has eigenvalues of the form,

$$f_3(\mu_i) = c_3\mu_i + b_3. \tag{9}$$

We start with,

$$\|f_3(A) - L_{rw}\|_2 \geq |f_3(\mu_i) - \eta_i| = |c_3\mu_i + b_3 - \eta_i|, \tag{10}$$

for $i \in \{1, 2, \ldots, n\}$ and $c_3 \leq 0$ (to ensure equal ordering in magnitude of the two compared spectra). Then,

$$\begin{aligned} \|f_3(A) - L_{rw}\|_2 &= \left\|c_3 A + b_3 I - I + D^{-1}A\right\|_2 \\ &= \left\|(c_3 D + I)D^{-1}A + b_3 I - I\right\|_2. &(11)\end{aligned}$$

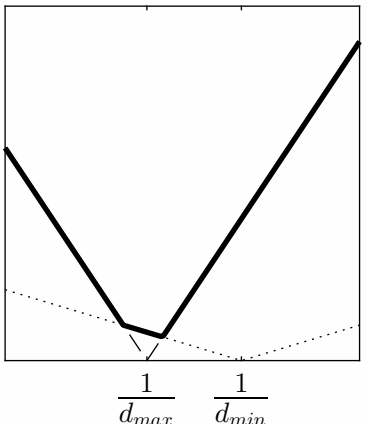


**Fig. 2.** This plot displays values of $c_2$ on the x-axis. The dotted line corresponds to the function $|d_{\min}c_2 - 1|$, the dashed line plots the function $|d_{\max}c_2 - 1|$ and the solid line depicts the bound which is to be minimised in (8), i.e., $\max(|d_{\max}c_2 - 1|, |d_{\min}c_2 - 1|)$.

At this stage we choose $b_3 \stackrel{\text{def}}{=} 1$ to simplify the norm. Then,

$$\|f_3(A) - L_{rw}\|_2 \leq \|I + c_3 D\|_2 \left\|D^{-1}A\right\|_2 \tag{12}$$

$$= \max\left(|1 + d_{\max}c_3|, |1 + d_{\min}c_3|\right), \tag{13}$$

where in (12) we use the fact that $\left\|D^{-1}A\right\|_2 = 1$ [4, p. 64]. Finding $c_3$ as the analytical minimum of this term is equivalent to finding $c_2$ in (8) and therefore $c_3 = -c_2 \stackrel{\text{def}}{=} -2/(d_{\max} + d_{\min})$. Consequently,

$$\|f_3(A) - L_{rw}\|_2 \leq \frac{d_{\max} - d_{\min}}{d_{\max} + d_{\min}}.$$

Hence, we obtain

$$|f_3(\mu_i) - \eta_i| \leq \frac{d_{\max} - d_{\min}}{d_{\max} + d_{\min}} \stackrel{\text{def}}{=} e\left(A, L_{rw}\right).$$

## 5 Proof of Theorem 4

*Proof.* The bound on the normalised eigengap difference of the adjacency matrix $A$ and the unnormalised Laplacian $L$, denoted $g(A, L)$, can be derived as follows:

$$\begin{aligned}
\left|\frac{\mathcal{M}_i}{2d_{\max}} - \frac{\mathcal{L}_i}{2d_{\max}}\right| &= \frac{1}{2d_{\max}}\left|\mu_i - \mu_{i+1} - \lambda_{i+1} + \lambda_i\right| \\
&= \frac{1}{2d_{\max}}\left|\mu_i - \frac{d_{\max}+d_{\min}}{2} + \lambda_i - \mu_{i+1} + \frac{d_{\max}+d_{\min}}{2} - \lambda_{i+1}\right| \\
&= \frac{1}{2d_{\max}}\left|[\lambda_i - f_1(\mu_i)] + [f_1(\mu_{i+1}) - \lambda_{i+1}]\right| \qquad (14) \\
&\leq \frac{1}{2d_{\max}} 2e(A, L) \qquad (15) \\
&= \frac{d_{\max} - d_{\min}}{2d_{\max}} \stackrel{\text{def}}{=} g(A, L),
\end{aligned}$$

where the triangle inequality has been used to go from (14) to (15).

We proceed to derive a bound on the normalised eigengap difference of $L$ and $L_{rw}$, denoted $g(L, L_{rw})$, as follows:

$$\begin{aligned}
\left|\frac{\mathcal{L}_i}{2d_{\max}} - \frac{\mathcal{N}_i}{2}\right| &= \frac{1}{2}\left|\frac{1}{d_{\max}}\left(\lambda_{i+1} - \lambda_i\right) + \eta_i - \eta_{i+1}\right| \\
&\leq \frac{1}{2}\left[\left|\frac{1}{d_{\max}}\lambda_{i+1} - \eta_{i+1}\right| + \left|\frac{1}{d_{\max}}\lambda_i - \eta_i\right|\right],
\end{aligned}$$

from the triangle inequality. A comparison with (6), shows that these eigenvalue differences can be bounded by replacing $c_2$ in (6) by $1/d_{\max}$ and then making this substitution into (8),

$$\begin{aligned}
\left|\frac{\mathcal{L}_i}{2d_{\max}} - \frac{\mathcal{N}_i}{2}\right| &\leq \frac{1}{2}\left[4\max\left(0, \left|\frac{d_{\min}}{d_{\max}} - 1\right|\right)\right] \\
&= 2\left(1 - \frac{d_{\min}}{d_{\max}}\right) \\
&= 2\frac{d_{\max} - d_{\min}}{d_{\max}} \stackrel{\text{def}}{=} g(L, L_{rw}).
\end{aligned}$$

Finally, we will derive the bound on the normalised eigengaps of $A$ and $L_{rw}$, denoted by $g(A, L_{rw})$.

$$\begin{aligned}
\left|\frac{\mathcal{M}_i}{2d_{\max}} - \frac{\mathcal{N}_i}{2}\right| &= \frac{1}{2}\left|1 - 1 + \frac{1}{d_{\max}}\left(\mu_i - \mu_{i+1}\right) + \eta_i - \eta_{i+1}\right| \\
&\leq \frac{1}{2}\left[\left|1 - \frac{1}{d_{\max}}\mu_{i+1} - \eta_{i+1}\right| + \left|1 - \frac{1}{d_{\max}}\mu_i - \eta_i\right|\right],
\end{aligned}$$

via the triangle inequality. Again, as in the proof of Theorem 3, we chose the translation parameter equal to 1 to simplify the norm. Then, a comparison with

(10), shows that these eigenvalue differences can be bounded by replacing $c_3$ by $-1/d_{\max}$ and then substituting into (13) to give

$$\left|\frac{\mathcal{M}_i}{2d_{\max}} - \frac{\mathcal{N}_i}{2}\right| \leq \max\left(0, \left|1 - \frac{d_{\min}}{d_{\max}}\right|\right)$$
$$= \frac{d_{\max} - d_{\min}}{d_{\max}} \stackrel{\text{def}}{=} g(A, L_{rw}).$$

## References

1. Bai, Z., Demmel, J., Dongarra, J., Ruhe, A., van der Vorst, H.: Templates for the solution of algebraic eigenvalue problems: a practical guide. SIAM (2000).
2. Horn, R.A., Johnson, C.R.: Topics in Matrix Analysis. Cambridge U.K.: Cambridge University Press (1991).
3. Lutzeyer, J.F., Walden, A.T.: Comparing Spectra of Graph Shift Operator Matrices. In: Cherifi, H., Gaito, S., Mendes, J.F., Moro, E., Rocha, L.M. (eds.) Complex Networks and Their Applications VIII, pp. 191–202. Springer, Cham (2020). https://doi.org/10.1007/978-3-030-36683-4_16
4. van Mieghem, P.: Graph Spectra for Complex Networks. Cambridge University Press, Cambridge U.K. (2011).